Electronic Supplementary Information (ESI)

for

Green Synthesis of 3D Cesium Lead Halide Perovskite Nanocrystals and 2D Ruddlesden-Popper Nanoplatelets in Menthol based Deep Eutectic Solvents

Shovon Chatterjee, Arghya Sen, and Pratik Sen*

Department of Chemistry, Indian Institute of Technology Kanpur, Kanpur – 208 016, UP, India

*Corresponding Authors, E-mail: psen@iitk.ac.in; Phone: +91 512 259 6312; FAX: +91 512 259 6806

Table of content:

High-resolution XPS of Pb 4f of CPB LAMe. (d) High-resolution XPS of Br 3d of CPB LAMe.

- **Figure S7:** Size distribution analysis of CPB NCs. (a) Size distribution of CPB-LAMe. (b) Size distribution of CPB-CAMe. (c) Size distribution of CPB-BAMe.
- **Figure S8:** Selected area electron diffraction (SAED) analysis of CPB NCs. (a) SAED analysis of CPB-LAMe. (b) SAED analysis of CPB-LAMe. (c) SAED analysis of CPB-LAMe.
- **Figure S9:** High resolution TEM (HRTEM) analysis of CPB NCs (a) HRTEM image of CPB-LAMe. (b) HRTEM image of CPB-CAMe. (c) HRTEM image of CPB-BAMe. (d) Fourier filter image of the selected area marked in yellow from figure SXa, where the right bottom inset shows the FFT of the selected area. (e) Fourier filter image of the selected area marked in yellow from figure SXb, where the right bottom inset shows the FFT of the selected area. (f) Fourier filter image of the selected area marked in yellow from figure SXc, where the right bottom inset shows the FFT of the selected area.
- **Table S1:** Time resolved PL fitting parameters of CPB-LAMe, CPB-CAMe and CPB-BAMe NCs.
- **Table S2:** Time resolved PL fitting parameters of CPB-LAMe and OAmBr treated CPB-LAMe NCs.
- **Figure S10:** Ambient PL stability of colloidal CPB-LAMe, CPB-CAMe, and CPB-BAMe NCs.
- **Figure S11:** (a) TEM image of pristine CPB NCs. (b) Size distribution of pristine CPB NCs.
- **Figure S12:** Steady state absorption (black spectrum) and PL (green) of pristine CPB.
- **Figure S13:** TEM images (a-c) of CPB-LAMe prepared at 75ºC keeping cesium to lead ratio unity.
- **Table S3:** Time-resolved PL fitting parameters of CPB-2D (n=3) and OAmBr treated CPB-2D (n=3) NPLs.
- **Figure S14:** Effect of OAmBr treatment on optical properties of CPB-2D (n=3) NPLs. (a) Comparative absorption spectra of CPB-2D (n=3) NPLs and OAmBr treated CPB-2D (n=3) NPLs. (b) Comparative PL spectra of CPB-2D (n=3) NPLs and OAmBr treated CPB-2D (n=3) NPLs. (c) Comparative PL transient at 460 nm of CPB-2D (n=3) NPLs and OAmBr treated CPB-2D (n=3) NPLs.
- **Figure S15:** SAED pattern of CPB-2D (n=3)

- **Figure S16:** X-ray photoelectron spectroscopic (XPS) analysis of CPB-2D (n=3). (a) Survey spectra of CPB-2D (n=3). (b) High-resolution XPS of Cs 3d of CPB-2D (n=3). (c) High-resolution XPS of Pb 4f of CPB-2D (n=3). (d) High-resolution XPS of Br 3d of CPB-2D (n=3).
- **Figure S17:** Ambient stability of CPB-2D (n=3).
- **Figure S18:** PXRD patterns of $CsPbCl_3$, $CsPb(Cl/Br)_3$, $CsPbBr_3$, $CsPb(Br/I)_3$, and $CsPbI_3$ NCs synthesized in LAMe.
- **Figure S19:** Size distribution of (a) $CsPbCl_3$, (b) $CsPb(Cl/Br)_3$, (c) $CsPb(Br/I)_3$, and (d) $CsPbI_3$ NCs (inset containing corner distance idea of hexagonal $CsPbI_3$ NCs.

Supporting data

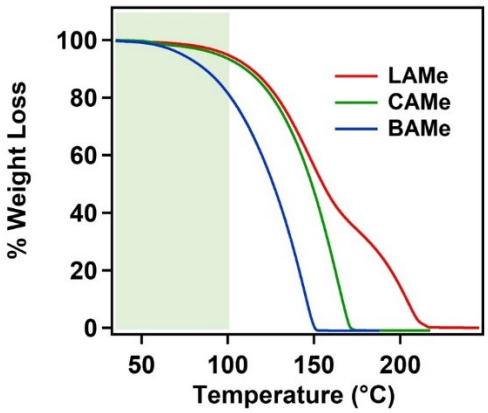

Figure S1: Thermogravimetric analysis (TGA) of the DES media.

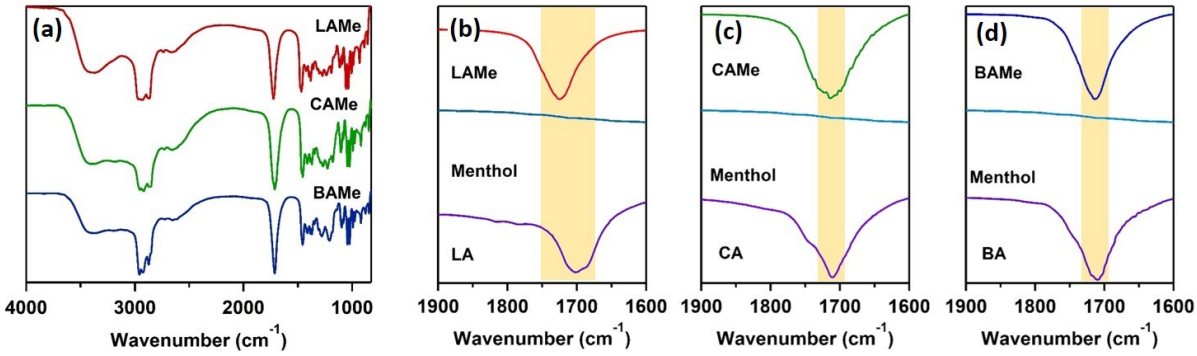

Figure S2: (a) IR analysis of the LAMe, CAMe and BAMe DESs. (b) IR spectra of lauric acid (LA), menthol and LAMe in the carbonyl region. (c) IR spectra of caprylic acid, menthol and CAMe in the carbonyl region. (d) IR spectra of butyric acid, menthol and BAMe in the carbonyl region. The carboxylic C=O characteristic of pure BA is observed at 1708 cm^{-1}, whereas it is observed at 1710 cm^{-1} and 1701 cm^{-1} for CA and LA, respectively. These peaks shift to 1714 cm^{-1}, 1719 cm^{-1}, and 1717 cm^{-1} in BAMe, CAMe, and LAMe, respectively, after the synthesis of DESs.

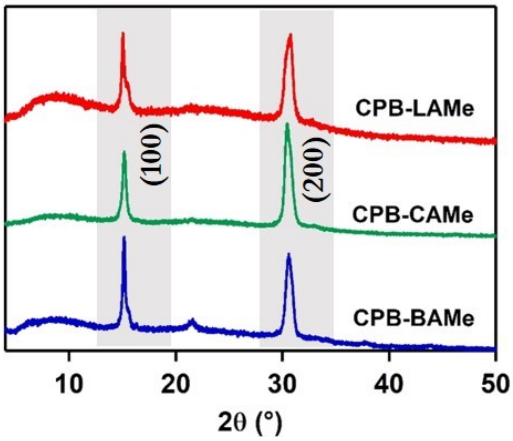

Figure S3. Powder X-ray diffraction (PXRD) pattern of CPB-LAMe (red), CPB-CAMe (green) and CPB-BAMe (blue).

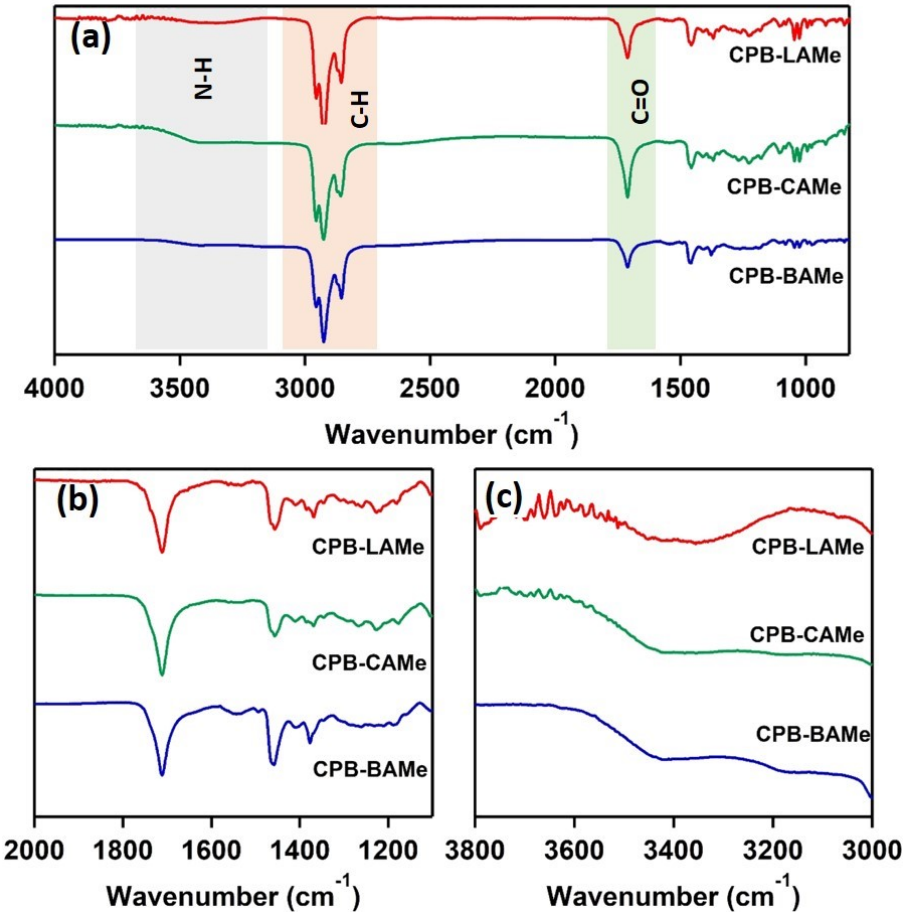

Figure S4. IR analysis of CPB NCs. (a) IR spectra of CPB-LAMe, CPB-CAMe and CPB-BAMe. (b) IR spectra of CPB-LAMe, CPB-CAMe and CPB-BAMe in carbonyl region. (c) IR spectra of CPB-LAMe, CPB-CAMe and CPB-BAMe in N-H stretching region.

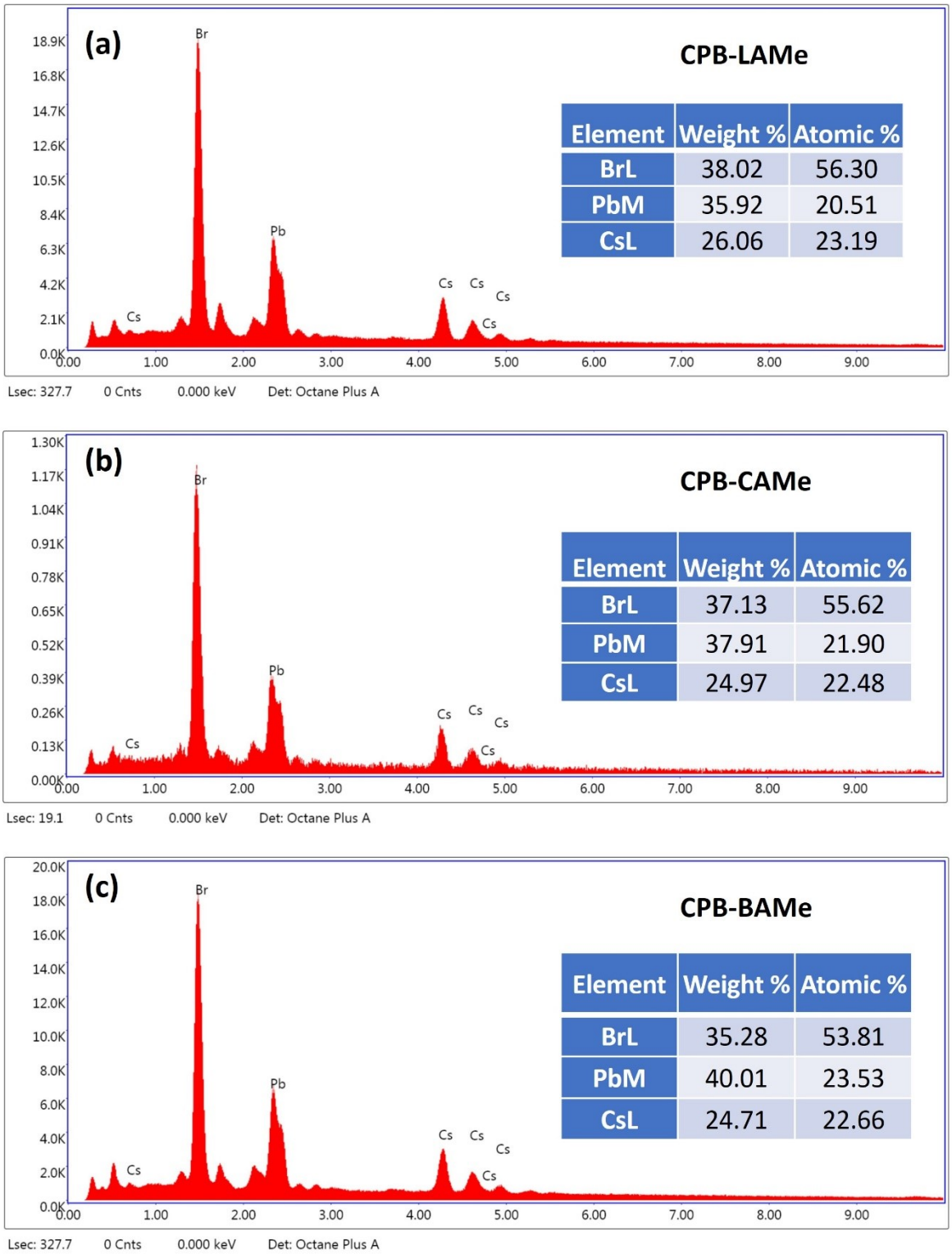

Figure S5. Energy dispersive X-ray spectra and elemental analysis of (a) CPB-LAMe, (b) CPB-CAMe and (c) CPB-BAMe.

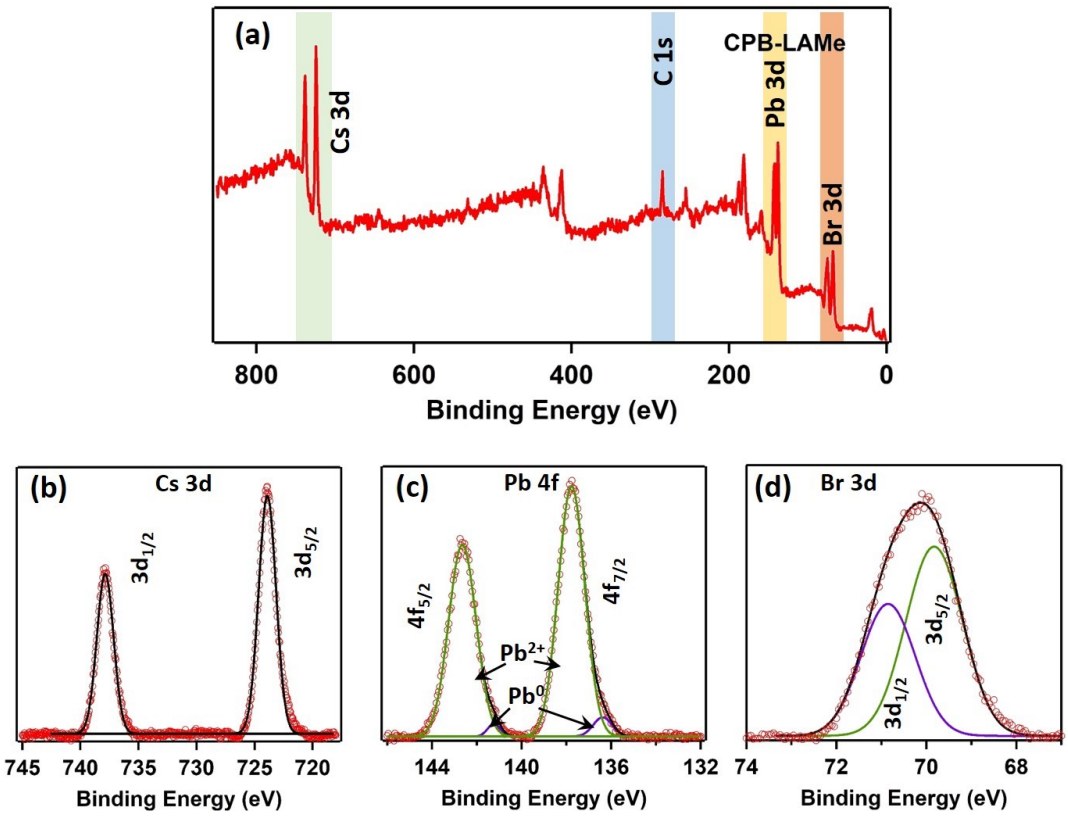

Figure S6: X-ray photoelectron spectroscopic (XPS) analysis of CPB LAMe. (a) Survey spectra of CPB LAMe. (b) High-resolution XPS of Cs 3d of CPB LAMe. (c) High-resolution XPS of Pb 4f of CPB LAMe. (d) High-resolution XPS of Br 3d of CPB LAMe.

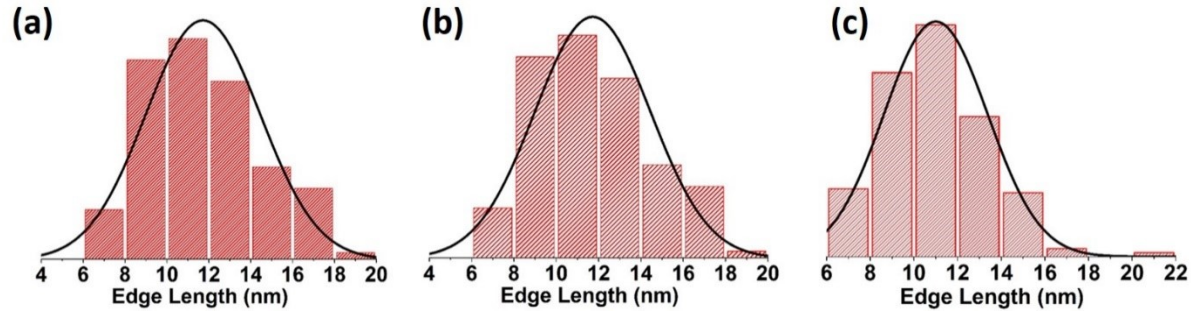

Figure S7: Size distribution analysis of CPB NCs. (a) Size distribution of CPB-LAMe. (b) Size distribution of CPB-CAMe. (c) Size distribution of CPB-BAMe.

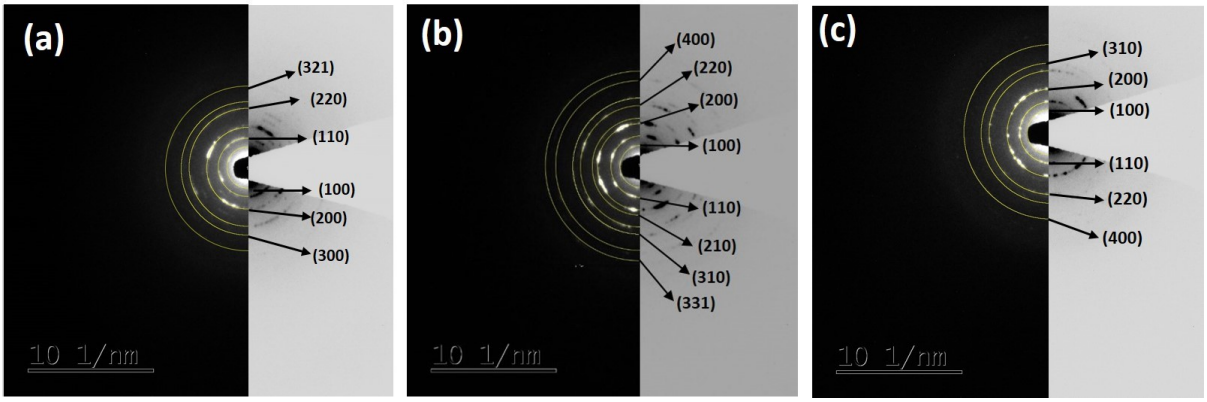

Figure S8: Selected area electron diffraction (SAED) analysis of CPB NCs. (a) SAED analysis of CPB-LAMe. (b) SAED analysis of CPB-LAMe. (c) SAED analysis of CPB-LAMe.

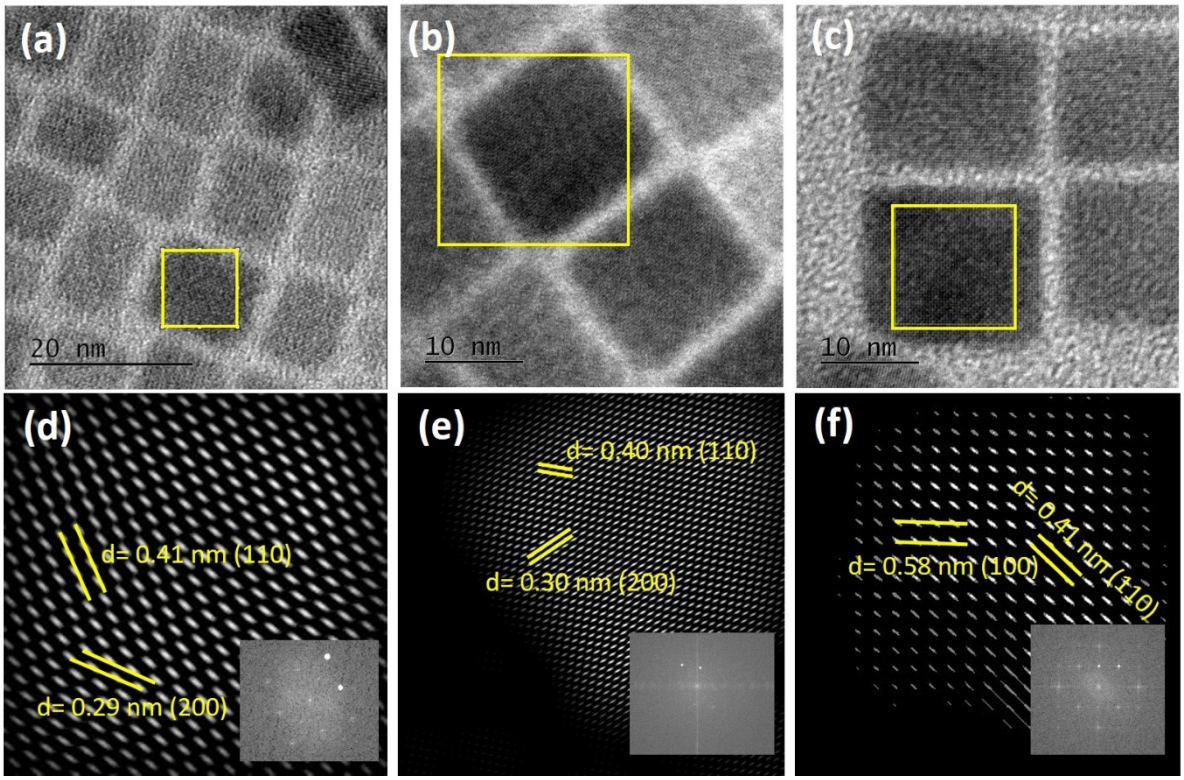

Figure S9: High resolution TEM (HRTEM) analysis of CPB NCs. HRTEM image of (a) CPB-LAMe. (b) CPB-CAMe (c) CPB-BAMe. The Fourier filter images of the selected area marked in yellow from (d) of figure S9a, (e) of figure S9b and (f) of figure S9c. The right bottom inset images in figure S9(d), S9(e) and S9(f) respectively represent the corresponding FFT of the selected area.

Table S1: Time resolved PL fitting parameters of CPB-LAMe, CPB-CAMe and CPB-BAMe NCs.

Sample	τ_1 (relative %)	τ_2 (relative %)	τ_3 (relative %)	τ_{avg}
CPB-LAMe	1.4 ns (25%)	6.1 ns (52%)	19 ns (23%)	13.1 ns
CPB-CAMe	1.3 ns (27%)	5.9 ns (51%)	19 ns (22%)	13.0 ns
CPB-BAMe	1.3 ns (30%)	6.0 ns (50%)	24 ns (20%)	17.7 ns

Table S2: Time resolved PL fitting parameters of CPB-LAMe and OAmBr treated CPB-LAMe NCs.

Sample	τ_1 (relative %)	τ_2 (relative %)	τ_3 (relative %)	τ_{avg}
CPB-LAMe	1.4 ns (25%)	6.1 ns (52%)	19 ns (23%)	13.1 ns
OAmBr treated CPB-LAMe		6.2 ns (63%)	20 ns (37%)	14.9 ns

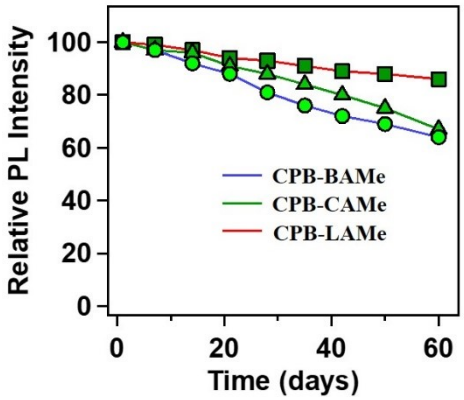

Figure S10: Ambient PL stability of colloidal CPB-LAMe, CPB-CAMe, and CPB-BAMe NCs.

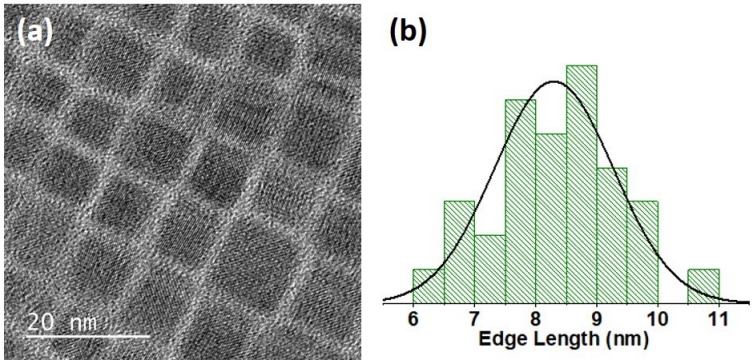

Figure S11: (a) TEM image of pristine CPB NCs. (b) Size distribution of pristine CPB NCs.

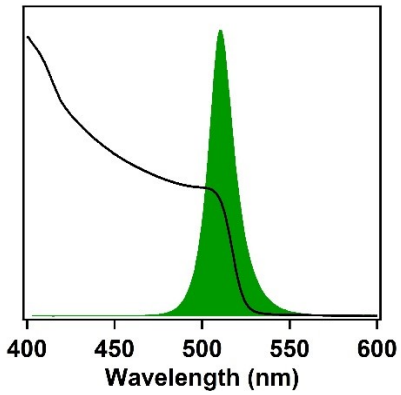

Figure S12: Steady state absorption (black spectrum) and PL (green) of pristine CPB.

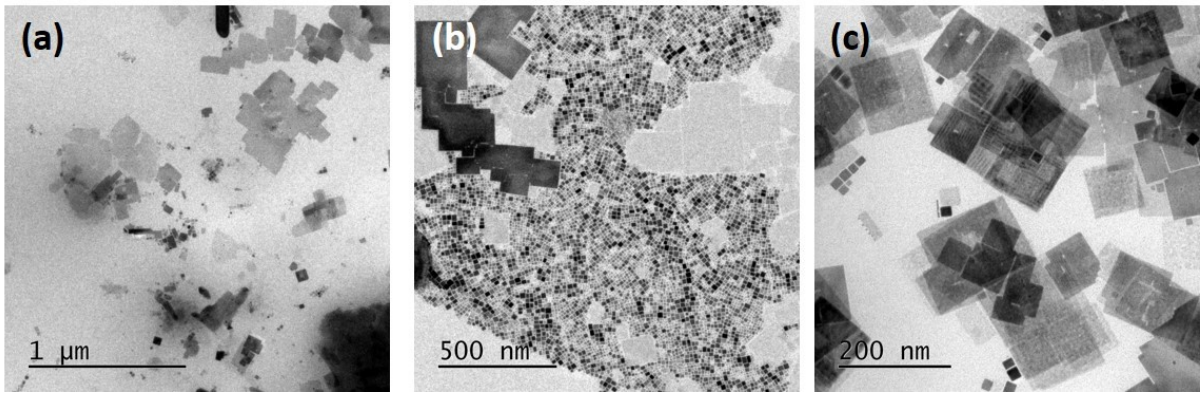

Figure S13: TEM images (a-c) of CPB-LAMe prepared at 75ºC keeping cesium to lead ratio unity.

Table S3: Time-resolved PL fitting parameters of CPB-2D (n=3) and OAmBr treated CPB-2D (n=3) NPLs.

Sample	τ_1 (relative %)	τ_2 (relative %)	τ_3 (relative %)	τ_{avg}
CPB-2D (n=3)	0.8 ns (38%)	3.4 ns (53%)	8.1 ns (9%)	4.3 ns
OAmBr treated CPB-2D (n=3)	1.1 ns (22%)	3.9 ns (64%)	9 ns (14%)	5.3 ns

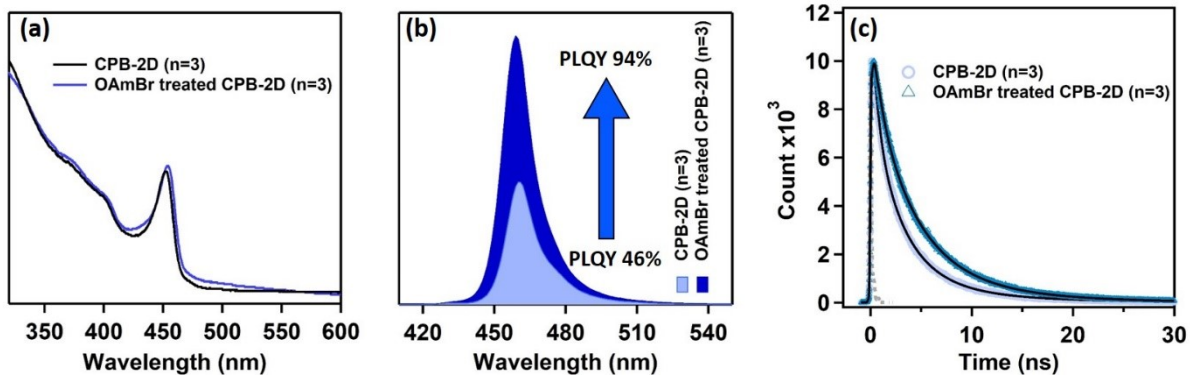

Figure S14: Effect of OAmBr treatment on optical properties of CPB-2D (n=3) NPLs. (a) Comparative absorption spectra of CPB-2D (n=3) NPLs and OAmBr treated CPB-2D (n=3) NPLs. (b) Comparative PL spectra of CPB-2D (n=3) NPLs and OAmBr treated CPB-2D (n=3) NPLs. (c) Comparative PL transient at 460 nm of CPB-2D (n=3) NPLs and OAmBr treated CPB-2D (n=3) NPLs.

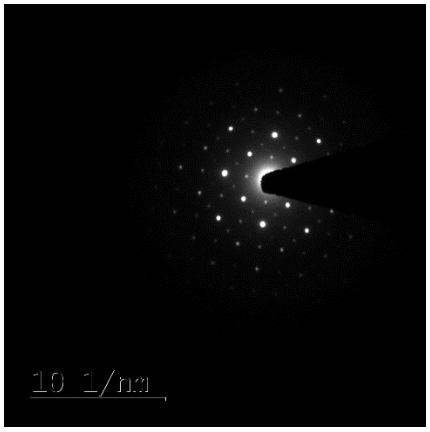

Figure S15: SAED pattern of CPB-2D (n=3)

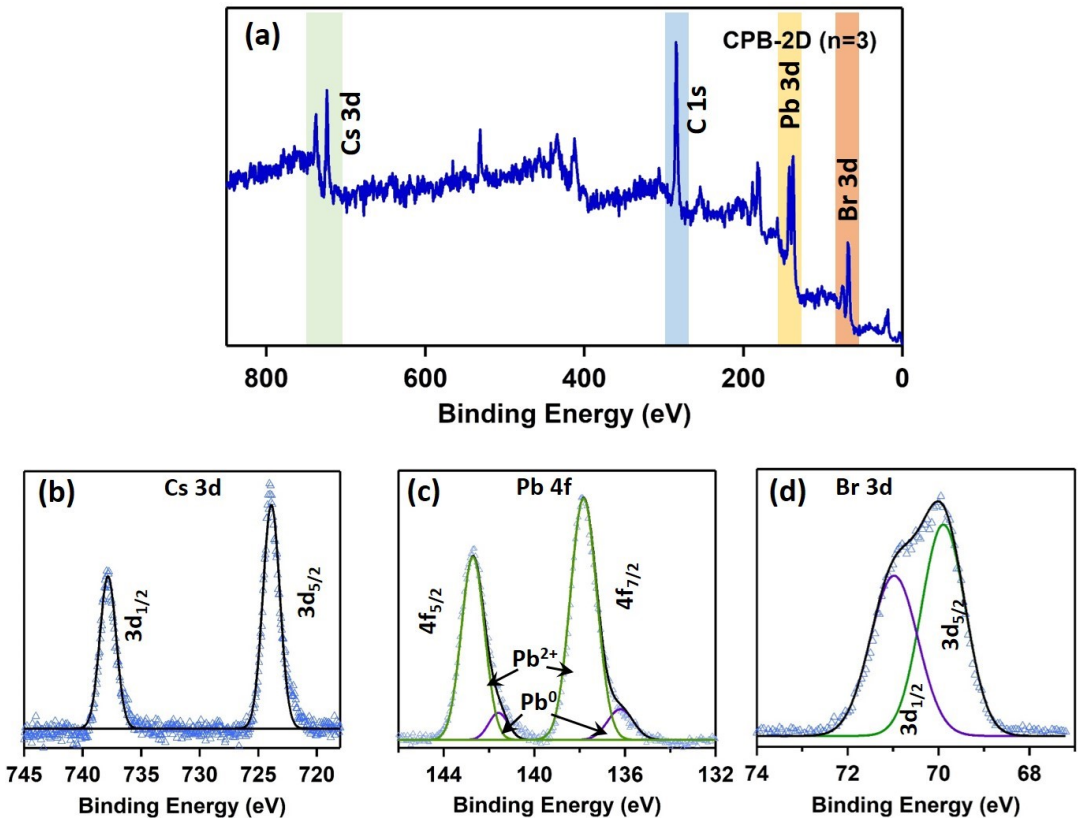

Figure S16: X-ray photoelectron spectroscopic (XPS) analysis of $(OAm)_2Cs_2Pb_3Br_{10}$ (CPB-2D (n=3)). (a) Survey spectra of CPB-2D (n=3). (b) High-resolution XPS of Cs 3d of CPB-2D (n=3). (c) High-resolution XPS of Pb 4f of CPB-2D (n=3). (d) High-resolution XPS of Br 3d of CPB-2D (n=3).

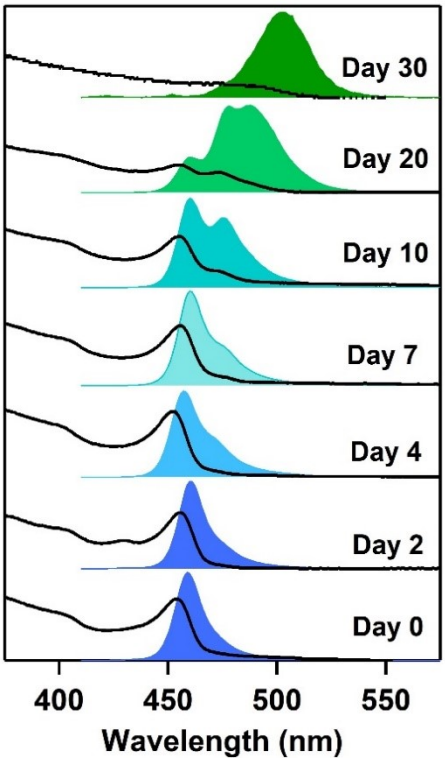

Figure S17: Ambient stability of CPB-2D (n=3).

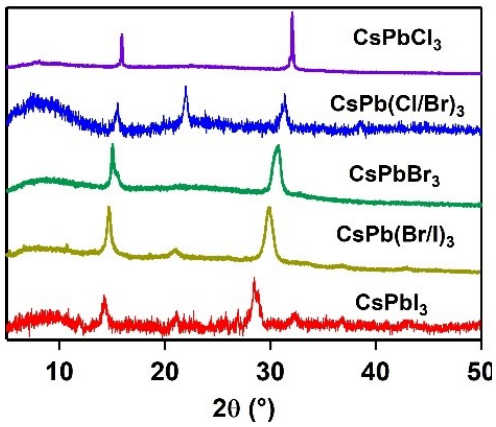

Figure S18: PXRD patterns of $CsPbCl_3$, $CsPb(Cl/Br)_3$, $CsPbBr_3$, $CsPb(Br/I)_3$, and $CsPbI_3$ NCs synthesized in LAMe.

Table S4: Time resolved PL fitting parameters of $CsPbCl_3$, $CsPb(Cl/Br)_3$, $CsPb(Br/I)_3$ and $CsPbI_3$ NCs.

Sample	τ_1 (relative %)	τ_2 (relative %)	τ_3 (relative %)	τ_{avg}
$CsPbCl_3$	0.3 ns (80%)	2.2 ns (11%)	12.6 ns (9%)	3.9 ns
$CsPb(Cl/Br)_3$	0.4 ns (49%)	3.2 ns (26%)	13.1 ns (25%)	10.6 ns
$CsPb(Br/I)_3$	0.9 ns (12%)	11.7 ns (28%)	24.2 ns (60%)	21.8 ns
$CsPbI_3$	0.6 ns (37%)	4.7 ns (26%)	24.4 ns (37%)	10.4 ns

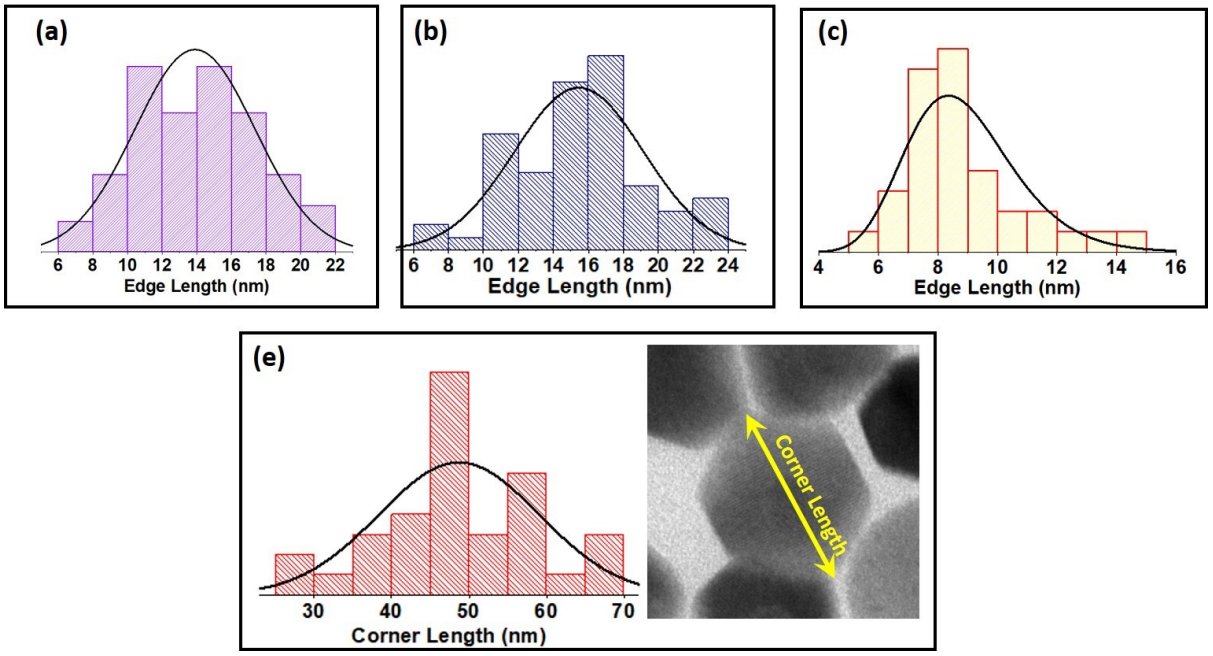

Figure S19: Size distribution of (a) $CsPbCl_3$, (b) $CsPb(Cl/Br)_3$, (c) $CsPb(Br/I)_3$, and (d) $CsPbI_3$ NCs (inset containing corner distance idea of hexagonal $CsPbI_3$ NCs.